Interspecies comparisons of Mg/Ca ratios in limpet shells

Niklas Hausmann[a,*], Donna Surge[b], Francisco Zangrando[c], Angelica Tivoli[c], Ivan Briz-Godino[d]

[a] *Leibniz Zentrum für Archäologie, Ludwig-Lindenschmit-Forum 1, Mainz, Germany, 55116*

[b] *University of North Carolina, 104 South Road, 225 Geology Building, Chapel Hill, NC, US, 27599-3315*

[c] *CONICET (Consejo Nacional de Investigaciones Científicas y Técnicas), Avenida Maipú 305, Ushuaia, Argentina, V9410BJA*

[d] *, Spain,*

Abstract

This study provides a short reassessment of the use of Magnesium to Calcium (Mg/Ca) ratios in Atlantic limpet shells to determine past sea surface temperatures. While *Patella vulgata* along the Spanish shoreline has since then repeatedly produced reliable correlations between sea surface temperature and Mg/Ca ratios, this is not the case for other patelloid species. *Patella vulgata* and *Nacella deaureata* have been studied using Mg/Ca with mixed or contrary results. In this study, we present elemental maps of various such species together with stable oxygen isotope values for some of the specimens. Our dataset also includes specimens that were previously unsuccessful in providing significant correlations between ^{18}O and Mg/Ca ratios. By reassessing these previous specimens and including a wider range of modern and archaeological samples from three patelloid species (*P. vulgata*, *N. deaureata*, and *N. magellanica*) we further add to the growing set of evidence for the reliable use of Mg/Ca ratios to detect palaeotemperature change and serve as a means to determine ontogenetic age and season of capture as well as to reveal locations of interest within the growth record (i.e. annual temperature minima and maxima) for the targeted analysis using ^{18}O or clumped oxygen isotope analysis.

Keywords: Sclerochronology, Limpets, Elemental Ratio, Mg/Ca

1. Introduction

Limpet shells are commonly found within archaeological sites and and past shorelines due to their robust carbonate structure and the long-term use of limpets as a marine food source. They have successfully been studied in the past in the context of coastal subsistence economies, site occupation on seasonal (Shackleton, 1973; Parker et al., 2018; Bosch et al., 2018) or long-term scale (Ortiz et al., 2015), as well as palaeotemperature (Fenger et al., 2007; Surge and Barrett, 2012; Wang et al., 2012; Colonese et al., 2012; Ferguson et al., 2011). Determining past sea surface temperature (SST) change largely relies on the measurement of ^{18}O-values within the calcitic parts of the shell, but attempts have been made to also use elemental ratios, such as magnesium to calcium (Mg/Ca), to have an alternative measure, that potentially provides a more accurate SST estimate than ^{18}O-values, which are also affected by changes in salinity. In addition, the data acquisition of elemental ratios — either through laser-ablation-isotope-ratio-mass-spectrometry (LA-ICP-MS) or laser induced breakdown spectroscopy (LIBS), can be much faster and cost-effective, increasing the number of specimens that can be studied overall (Durham et al., 2017; Hausmann et al., 2023).

*Corresponding author

Email address: niklas@palaeo.eu (Niklas Hausmann)

Problematically, links between Mg/Ca ratios and SST changes in many marine mollusc shells, including limpets, have shown to be unreliable (Surge and Lohmann, 2008; Wanamaker et al., 2008; Schöne et al., 2010; Freitas et al., 2012; Graniero et al., 2015; Poulain et al., 2015; Vihtakari et al., 2017). This is particularly the case where there is little available additional information on metabolic processes, organic components of the shell matrix, intra-increment and intra-shell variability, and growth rates, which can independently and unpredictably affect Mg/Ca ratios and confound their interpretation as temperature proxy. Confusingly, multiple different temperature equations have been found for the same species (see (Freitas et al., 2012; Vihtakari et al., 2017) and references therein). Coeval specimens sharing one locality can also show differences in their relation to SST (Hausmann et al., 2019). Where the use of Mg/Ca as a palaeotemperature proxy was successful, anomalous patterns in some specimens had still to be filtered out by hand, reducing the overall robustness of the results of those successful studies (Ferguson et al., 2011).

While recent research particularly of *Patella* sp. in the Mediterranean and Southwest Europe have provided promising results (Hausmann et al., 2019; García-Escárzaga et al., 2015, 2018). There remains a lack of clarity for Atlantic limpet species, particularly since it was last shown here, that they are not reliable recorders of palaeotemperature (Graniero et al., 2015).

In this study we will repeat and expand the analysis of Atlantic limpets to determine the reliability of Mg/Ca ratios as palaeotemperature proxies. To do this, we sampled a set of previously published and unpublished limpet specimens dating to modern and archaeological contexts using LIBS. LIBS allows us to carry out 2D imaging of entire shell sections, which helps us to navigate the complex elemental structure of the shell and better separate the external, temperature-related changes from the internal and less understood factors that influence the Mg/Ca ratio.

By relying and adding onto published datasets, we were able to simultaneously avoid costs for new high-resolution ^{18}O-data, to use real-world examples, and to also provide pilot-data for areas of existing research interest. Generally establishing the usefulness and reliability of Mg/Ca as SST proxy in limpets should help to provide a platform for future research and an important stepping stone to better understand elemental ratios in other marine mollusc shells.

2. Materials and Methods

2.1. Limpet specimens

2.1.1. Modern specimens

The analysed specimens, their origin and respective studies with research background information can be found in Table 1. Here we will briefly summarise their contextual information, which can be accessed in more detail at the respective studies (Nicastro et al., 2020; Surge and Barrett, 2012; Graniero et al., 2017). While those studies also included other specimens, their accessibility or state of preservation did not all lend them to be re-analysed.

Table 1: Overview of the modern and archaeological limpet specimens analysed in this study.

Context	Study	Species	Location	Sample ID	Previous analyses
Modern	(Nicastro et al., 2020)	*N. deaureata*	Cambaceres Bay - Tierra del Fuego (AR)	ND-1016-3	Stable oxygen and carbon isotope analysis
				ND-1016-4	
		N. magellanica		NM-1016-1	

Context	Study	Species	Location	Sample ID	Previous analyses
	(Graniero et al., 2017)	*P. vulgata*	Rack Wick Bay - Westray (UK)	NM-1016-3 ORK-LT5	Stable oxygen and carbon isotope analysis; Mg, Li, Sr, Ca,.
Archaeological	(Surge and Barrett, 2012)	*P. vulgata*	Rack Wick Bay - Westray (UK)	QG1-7188-1	Stable oxygen and carbon isotope analysis
				QG1-7189-2 QG2-1061-1 QG2-1064-1 QG2-7180-1 QG2-7180-2 QG1-7246-1	
	This study	*N. magellanica*	Heshkaia 35 in Moat Bay - Tierra del Fuego (AR)	Heshkaia_35-1	*none*
		N. deaureata		Heshkaia_35-2	
		N. deaureata		Heshkaia_35-3	
		N. magellanica		Heshkaia_35-4	
		N. magellanica		Heshkaia_35-5	
		N. magellanica		Heshkaia_35-6	
		N. magellanica		Heshkaia_35-7	
		N. deaureata		Heshkaia_35-8	
		N. magellanica		Heshkaia_35-9	

There are two main locations that we sourced specimens from: the Beagle Channel in Tierra del Fuego (Argentina) and the island of West Ray in Orkney (UK). Four specimens were collected from the Beagle Channel in Cambaceres Bay in October 2016. The area receives around 570 mm precipitation but the channel waters are predominantly influenced by marine currents and in the period of October 2015 to October 2016 stayed around 30.7 ± 0.7 psu (Nicastro et al., 2020). SSTs range from 4.7°C in August to 10°C in February.

On Westray one modern shell (ORK-LT5) was collected in Rack Wick Bay in August 2009. Westray lies about 70 km north of the Scottish mainland and experiences virtually no freshwater input with salinity values of 34.0 – 34.5 psu (Inall et al., 2009). The annual SST ranges from 6.3°C in March to 13.8°C in August (Figure 1).

2.1.2. Archaeological specimens

In total, we studied 16 archaeological specimens. Of those, seven *P. vulgata* come from Quoygrew on Westray dating to 900 – 1200 CE. These shells have previously been studied to characterise seasonal temperature change during the Medieval Climate Anomaly and the Little Ice Age (Surge and Barrett, 2012). Together they show a range of lifespans, with some comparatively long for their size (QG1-7246-1, 12 years within 16 mm of growth) making them particularly susceptible to time-averaging. That said, the majority are under 5 years old. These shells are an ideal comparative dataset from an archaeological assemblage to compare to the modern shell ORK_LT5 (Graniero et al., 2017).

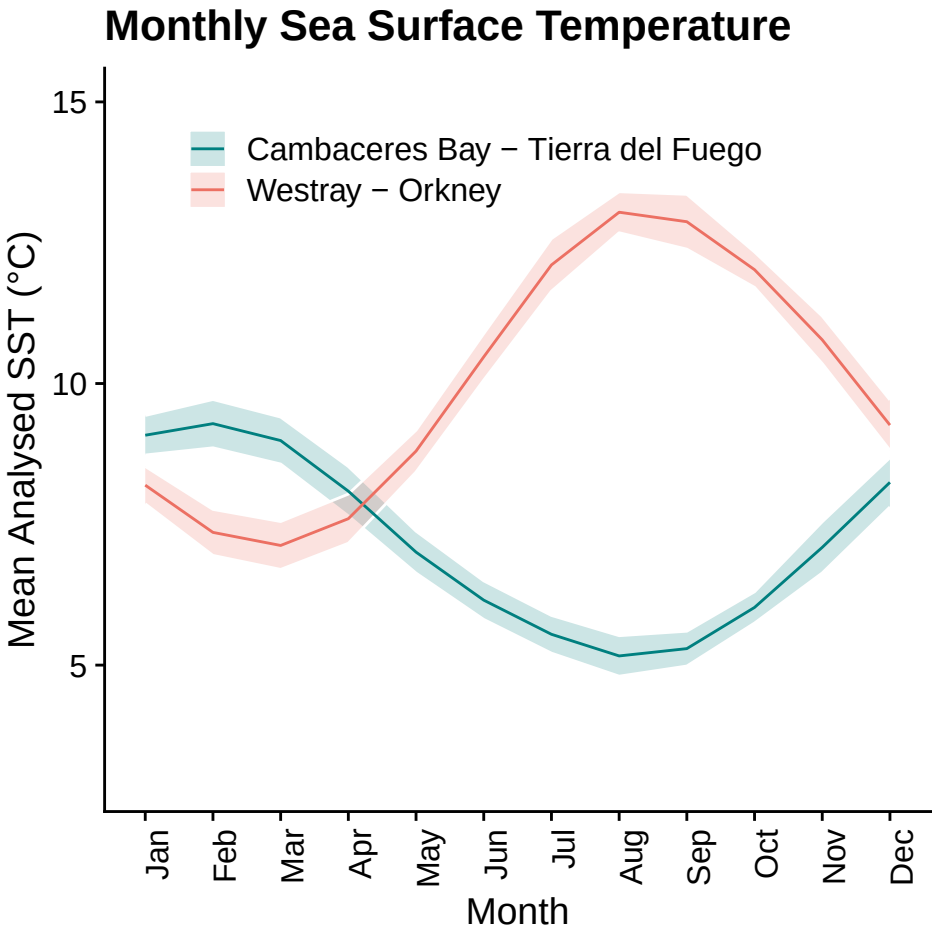

Figure 1: SST values averaged from years. SST values were sourced from Good et al. (2020)

Nine additional shells of *N. magellanica* (n=6) and *N. deaureata* (n=3) have been selected for LIBS analysis only, to provide a comparative dataset to the modern *Nacella* sp. shells. These have not been analysed for ^{18}O-values, but rather as a test to see whether patterns visible in the modern Mg/Ca ratio distributions are also preserved and apparent in the archaeological shells. They derive from the site of Heshkaia 35 situated within Moat Bay, around 30 km east of where the modern specimens in our study were collected (Zangrando et al., 2014, 2021). With radiocarbon dates putting the shells into the Late Holocene (1300 – 1450 CE) they are of similar age — if somewhat younger — as the assemblage from Quoygrew.

2.2. Methods

2.2.1. Mg/Ca ratios

Mg/Ca elemental imaging was carried out using Laser Induced Breakdown Spectroscopy at the Leibniz Zentrum für Archäologie (Mainz-Germany) using previously published methods (Hausmann et al., 2023). These involve the ablation of the shell section using an infrared (1064 nm) laser (1–2 mJ, 100 Hz) onto a surface area of 20–30 µm to generate a plasma plume. This plume emits light, which is measured using a synchronised spectrometer. The resulting light spectrum quantifies the emission lines of magnesium (MgII; 279.553 nm) and calcium (CaII; 315.887 nm) to determine their intensity ratio. While these two peaks alone do not represent the molar concentrations of both elements (as opposed to calibration free LIBS; e.g. (Martínez-Minchero et al., 2022)), the intensity ratio is linearly correlated to the molar concentration (Hausmann et al., 2017) and can be used as a reliable indicator of Mg/Ca changes within the shell carbonate.

Using this system we carried out elemental imaging of the shell specimens at a resolution of 50 µm distance between sampling spots. Each spot was irradiated 10 times with the 3 first spectra used for cleaning steps and the remaining summed to get an average Mg/Ca intensity ratio for each sample spot. Subsequently, we re-sampled the section using a line scan at 10 µm resolution. This leads to an overlap between sample spots, but also allows for a continuous record without gaps. Intensity ratios were filtered for cases with high relative standard deviation (i.e. more than 10%). These occurred in places where the previous sampling procedures for carbonate powder as part of the oxygen isotope analysis left an uneven sample surfaces introducing variability in the plasma generation and thus uncertainty in the data of these locations.

2.2.2. Oxygen isotopes

High-quality oxygen isotope values (^{18}O) were acquired from previous publications on *P. vulgata* (Surge and Barrett, 2012; Graniero et al., 2017), *N. deaureata* and *N. magellanica* (Nicastro et al., 2020), in which detailed descriptions of the stable isotope analysis methodology can be found. In short, all shells were sectioned along the main growth axis to expose the internal growth structure. From the exposed section carbonate powder samples were acquired using a micromill with resolutions of 100–200 µm and by targeting the calcitic M+2 layer of the shells. Analytical precision of the isotope values was consistently at 0.05–0.10‰ and values are reported in per mil units (‰) relative to the VPDB (Vienna Pee Dee Belemnite) standard.

Figure 2 and Figure 3 show the previously acquired sequential ^{18}O-values of limpet shells by species. Due to the high sampling resolution, all shells show seasonally resolved and multi-year quasi-sinusoidal records of SST change , with *Nacella* sp. shells living 2–3 years and *Patella v.* regularly over 3 years. In those instances where longer lifetimes are encountered (i.e. specimen QG1-7246-1, Figure 3 b). Interestingly, the annual ranges in ^{18}O-values are not similar between the coeval *Nacella* sp. specimens with ^{18}O values for the previous summer temperatures ranging from 0.4‰ to above 1.0‰, and for winter values between 2.7‰ and 2.0‰. *P. vulgata* has similarly variable ^{18}O-values for summer and winter seasons, alas the lack of more that one modern specimens, means that we cannot quantify the variability of recorded annual ranges between specimens.

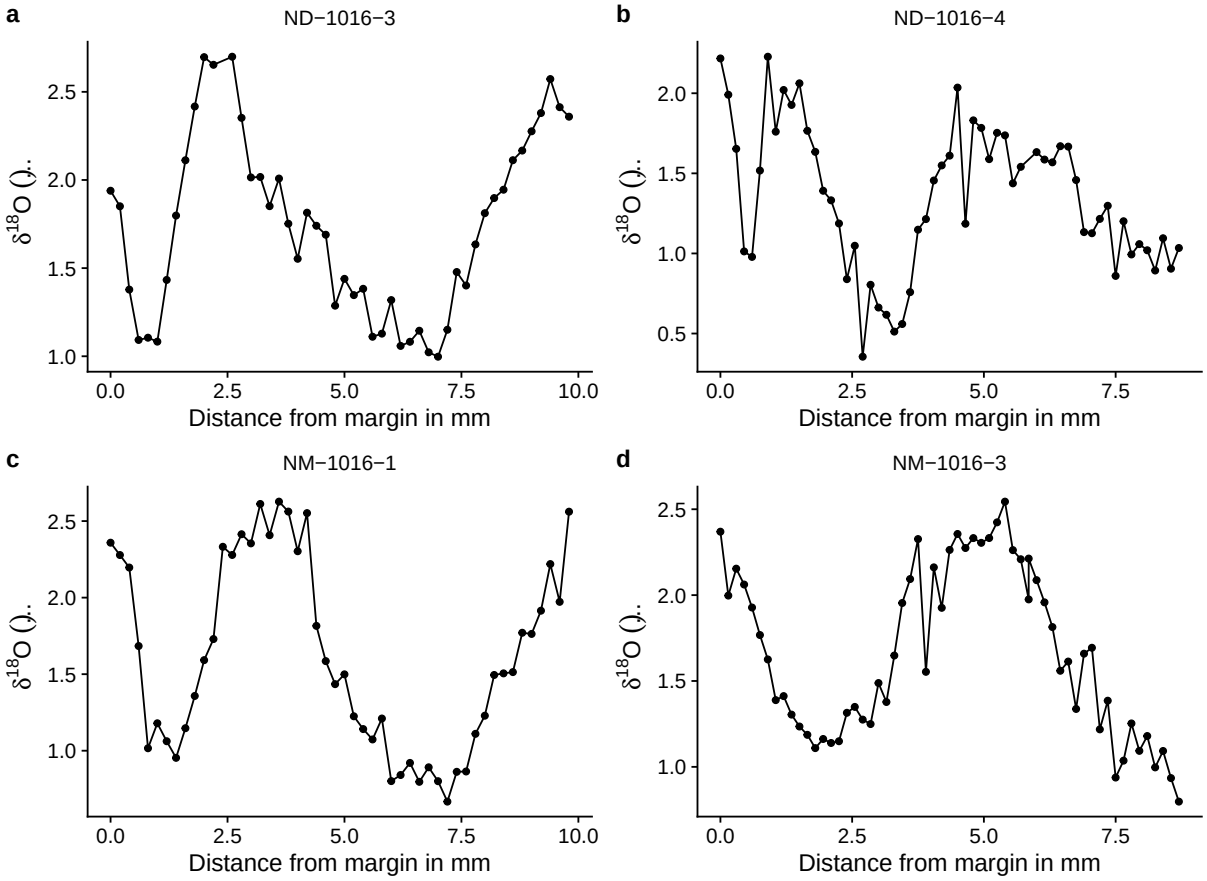

Figure 2: Isotope values of *Nacella* sp. limpet shells from Cambaceres Bay (*a-f*).

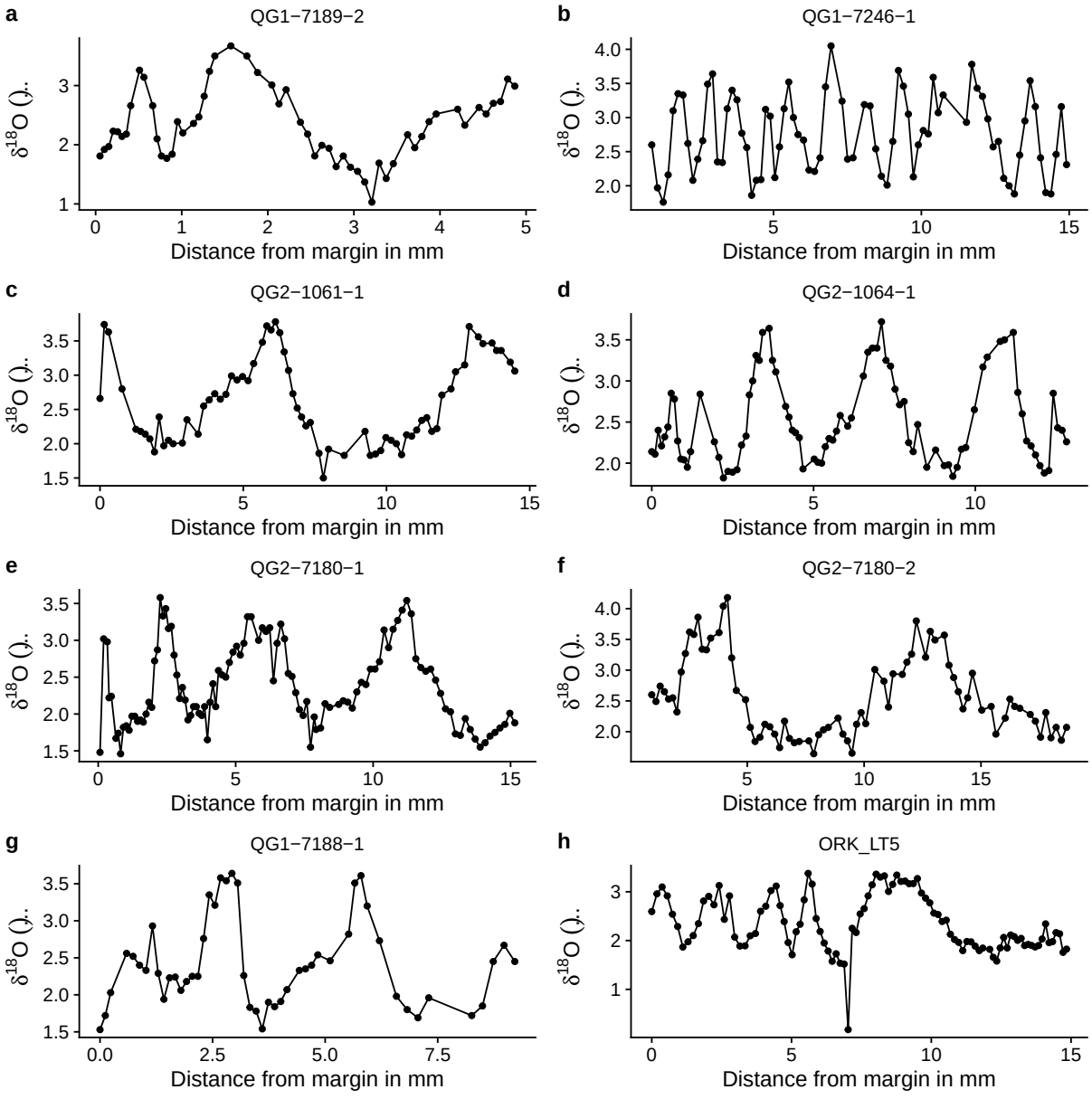

Figure 3: Isotope values of *Patella vulgata* limpet shells from Quoygrew (QG, *a-g*) and Rack Wick Bay (ORK, *h*) on Westray, Orkney.

2.3. Dynamic Time Warping

Because the exact location used in the analysis of stable oxygen isotopes is not possible to reconstruct for each carbonate powder sample, we used dynamic time warping (DTW) to align the time series of ^{18}O-values and Mg/Ca ratios. DTW is an algorithm that measures similarity between two proxy-sequences, which may vary in sampling resolution or interval. By stretching or compressing sections of the series, DTW finds the probable alignment between the two sequences. This allows us to compare the proxy data sets more effectively, ensuring that the temporal dynamics of each shell are accurately matched despite possible discrepancies in sampling intervals or rates. We applied the DTW algorithm using the `dtw` package in R (Giorgino, 2009; R Core Team, 2020), which provides a robust framework for aligning time series data. This involved selecting appropriate distance measures and constraints to ensure meaningful alignment. The process involved iterative adjustments to minimise the overall distance between corresponding points in the two data sets. The code used for this analysis as well as the data required to run it can be found in this **OSF repository**.

3. Results

3.1. Patella vulgata

The elemental imaging of *P. vulgata* shells consistently showed repeating patterns of Mg/Ca intensity ratio changes with high Mg/Ca intensity ratios indicating and low ratios indicating low temperature periods. As examples, Figure 4 shows the 2D-distribution of elemental ratios across the entire section of ORK-LT5 and the preserved anterior side of QG1-7188-1 (additional maps can be found in the supplementaries). The repeating patterns are found across the calcitic layers that are exterior to the myostracum (layers m+2 and m+3) as well as the layers that are interior (m-2) (Fenger et al., 2007). The layer m-1, which is also interior, consists of aragonite and is seen in Figure 4 in grey, as its Mg/Ca intensity ratio consistently falls below the range of interest (0.2 and above). Compared to other patelloid shells, whose interior is almost entirely made of aragonite, this layer is very thin.

Both specimens in Figure 4 show increased Mg/Ca intensity ratios towards the outside of the shell and some degree of intra-increment variability. This is particularly visible in Figure 4 c, where Mg/Ca intensity ratios range from ~0.5–0.7 in the first year of growth (9–12 mm on the y-axis). A similar pattern is visible in the interior m-2 layer of ORK-LT5 (Figure 4 a), which increase towards the anterior of the shell (0–10 mm on the x-axis).

Line scans also indicate well the quasi-sinusoidal change of Mg/Ca intensity ratios expected based on the stable isotope data and elemental-imaging. That said, some of the variability of Mg/Ca intensity ratios within one season such as the summer period of QG1-7188-1 between 0.5 and 2.0 mm distance to the shell edge (@fig-Pat_LIBS d), is visible in a more dramatic manner than it appears in the 2D-image, showing the downside of line-scanning as opposed to the broader milling approach used for the analysis of carbonate powder (Ferguson et al., 2011).

Figure 5 shows the line scan of ORK-LT5 in comparison to its ^{18}O-values (similar graphs for other specimen can be found in the supplementaries). The measurements of the distance to the shell edge are not entirely identical, most likely because one growth increment can have several different distances. Depending on where one measures the distance and a line scan towards the interior would be shorter than a line scan towards the exterior. That said, increases and decreases of both proxies seem to mirror each other and to be well aligned.

Aligning the records programmatically using dynamic time warping, allowed us to compare them directly to determine specimen-specific equations and quantify the correlation of both proxies (Figure 6). The equations for all specimens are different but the majority (barring one: QG1-7246-1) do seem to cluster around shared parameters ($^{18}O = 0.6 - 0.065 * Mg/Ca$). The various coefficients of determination (R^2) range between

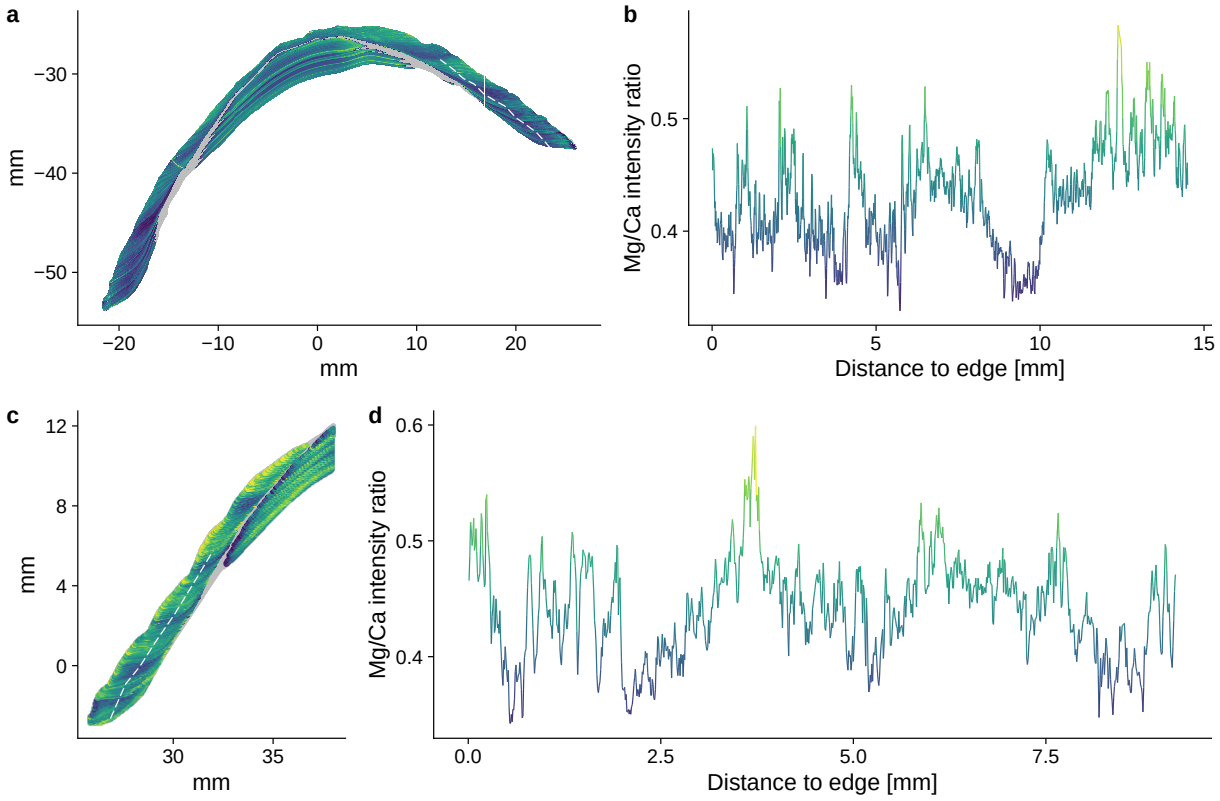

Figure 4: Example LIBS maps and line scans of analysed specimens. (a+b) ORK-LT and (c+d) QG1-7188-1. Note that the ranges of Mg/Ca intensity ratios are not identical but are chosen arbitrarily to increase contrast. Areas in grey consist of low-Mg aragonite and fall outside the chosen colour-range.

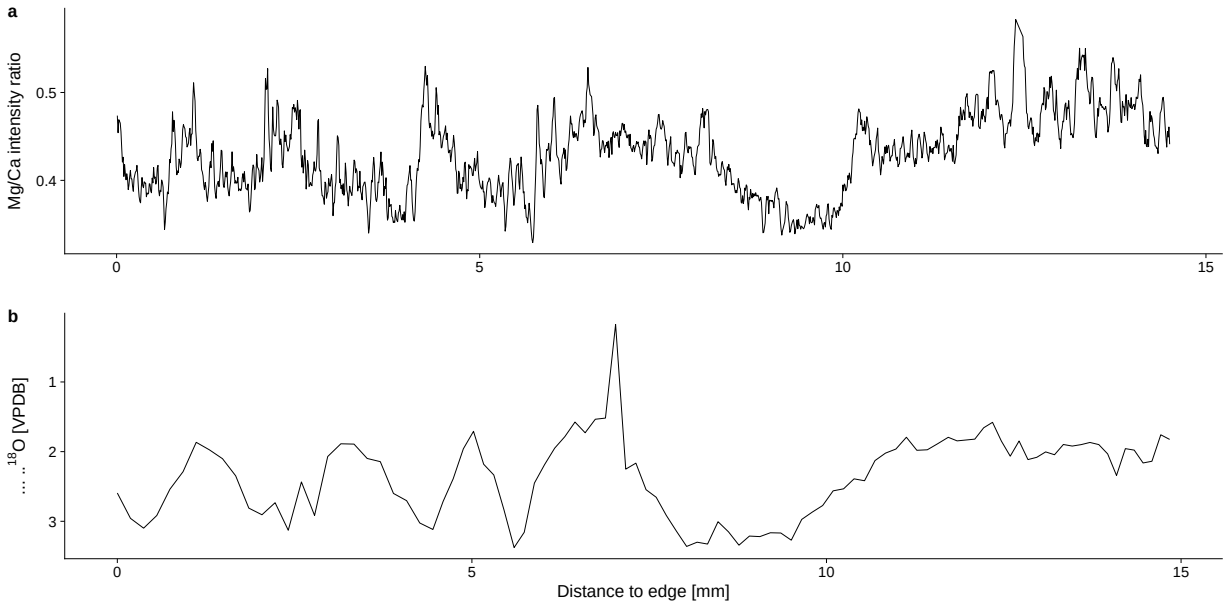

Figure 5: Comparison of LIBS line-scan and sequential ^{18}O-values of specimen ORK-LT5

0.81 (QG1-7246-1) and 0.95 (QG1-7189-2). These specimens are also the oldest and youngest, respectively, specimens, suggesting that lower growth rates and time averaging had a negative effect on the correlation of both proxies. The mean R^2 value is 0.89, suggesting a generally good fit between the two proxies.

3.2. Nacella *sp.*

The LIBS data for *Nacella* sp. specimens is less straightforward with shells being much thinner and thus patterns being more difficult to make out. Both specimens (ND-1016-3 and NM-1016-3) shown as example in Figure 7 (see additional graphs in supplementaries) also experience increases of Mg/Ca intensity ratio towards the exterior of the shell, similar to the *P. vulgata* specimens from Orkney. This intra-increment heterogeneity combined with the thinness of the shell, further complicates their analysis compared to *P. vulgata* or other *Patella* species (Hausmann et al., 2019). Nevertheless, repeating patterns were visible in the anterior section of the shell, which were also mirrored in the inner layers (m-2) of specimens NM-1016-3 (Figure 7 c).

Interestingly, the Mg/Ca intensity ratios in the *Nacella* sp. shells were much lower (0.05–0.30) than those seen in other patelloid species (e.g. 0.3–0.7 in *Patella vulgata* above, or 0.5–1.5 in) using the same emission lines. This is particularly visible in Figure 7 c, where Mg/Ca intensity ratios range from ~0.5–0.7 in (Hausmann et al., 2023)). While the intensity ratio depends chiefly on the chosen emission lines to calculate the proportion of the chosen Magnesium to the Calcium peak, the low ratios still indicate lower concentrations than seen elsewhere, or seen only in aragonitic parts of e.g. *Patella* shells.

Line scans reflect well the changes previously indicated by ^{18}O values and also indicate about two years of recorded growth. That said, the 2D imaging suggests that in both specimens a third summer can be added to the total record, which is not captured by the line scans. The variability seen in the *P. vulgata* specimens above is not as strong, which might also be related to the fast and consistent growth rate of the shells.

Figure 8 shows the line scans of ND-1016-3 and NM-1016-3 in comparison to their ^{18}O-values (similar graphs for the other *Nacella* sp. specimen can be found in the supplementaries). Compared to the *P. vulgata* records, these mirror each other much more clearly, due to the brief period recorded in the shells and its simple make-up.

The *Nacella* sp. specimens showed similarly clustered correlations, which interestingly were not grouped by species. In fact, specimens ND-1016-3 (*Nacella deaureata)* and NM-1016-3 (*Nacella magellanica*) are almost identical in their fitted equations (Figure 9). Both also share a high coefficient of determination (R^2) of 0.95 and 0.92 respectively, with the remaining specimens being somewhat lower (R^2 = 0.76 for ND-1016-4 and R^2=0.84 for NM-1016-3). The mean R^2 value for each *Nacella* species is 0.86 for *Nacella deaureata* and 0.88 for *Nacella magellanica*. Why two specimens of different species are so well aligned is not entirely certain and randomness cannot for now be ruled out. That said, since they both have a high R^2 value, it might just be that they were both minimally affected by factors other than SST, including the sampling location of our line scans.

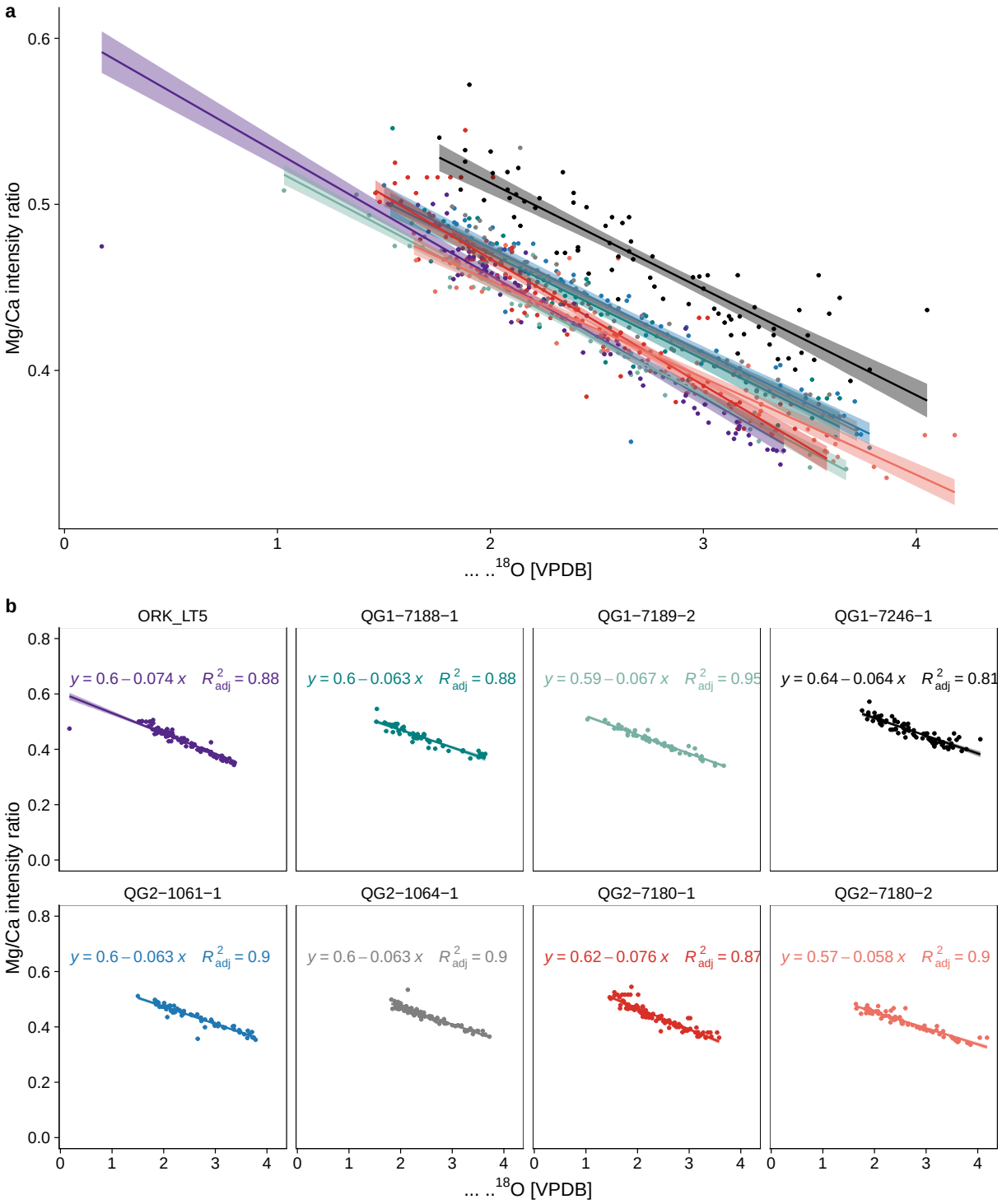

Figure 6: Correlation graphs for *Patella vulgata* specimens.

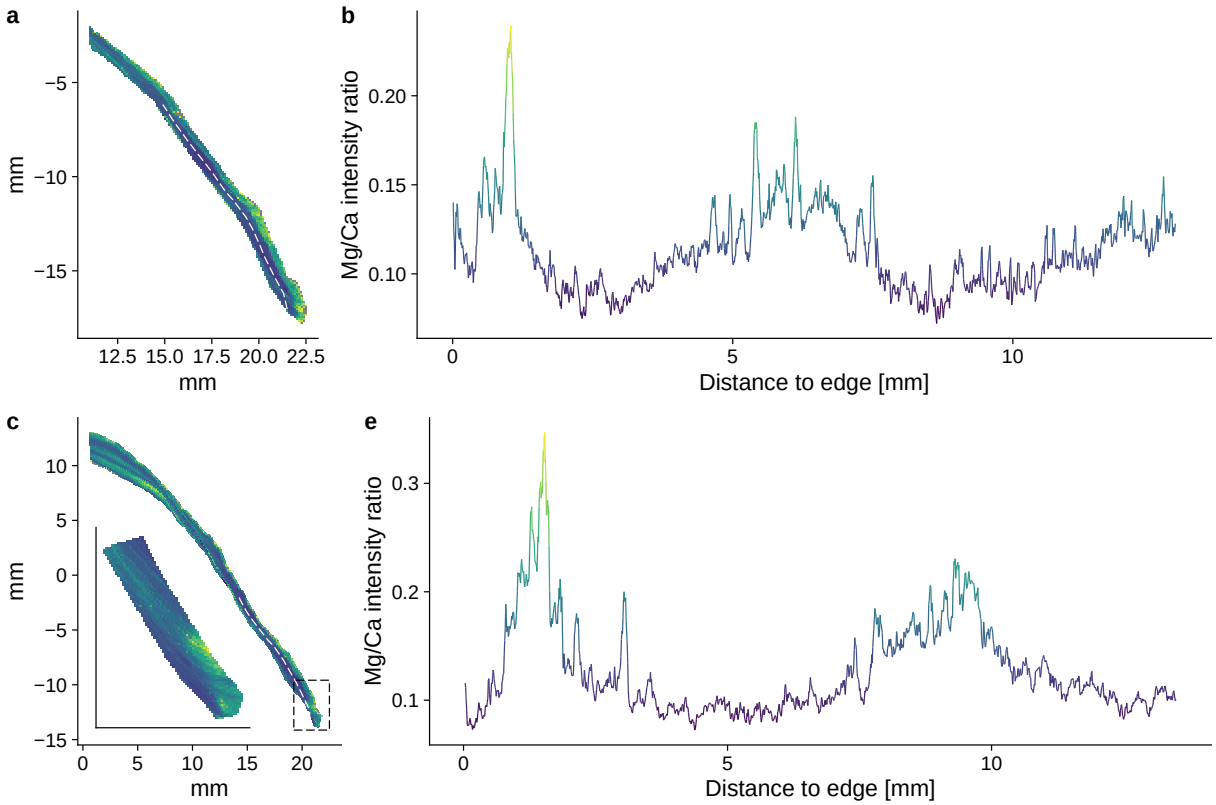

Figure 7: Example LIBS maps and line scans of analysed specimens. (a+b) ND-1016-3 and (c+d) NM-1016-3. Note that the ranges of Mg/Ca intensity ratios are not identical but are chosen arbitrarily to increase contrast. Areas in grey consist of low-Mg aragonite and fall outside the chosen colour-range. Note the inset in (c) where the shell edge has been resampled using a higher resolution (50 µm instead of 100 µm) to better understand the Mg/Ca ratios at the shell edge.

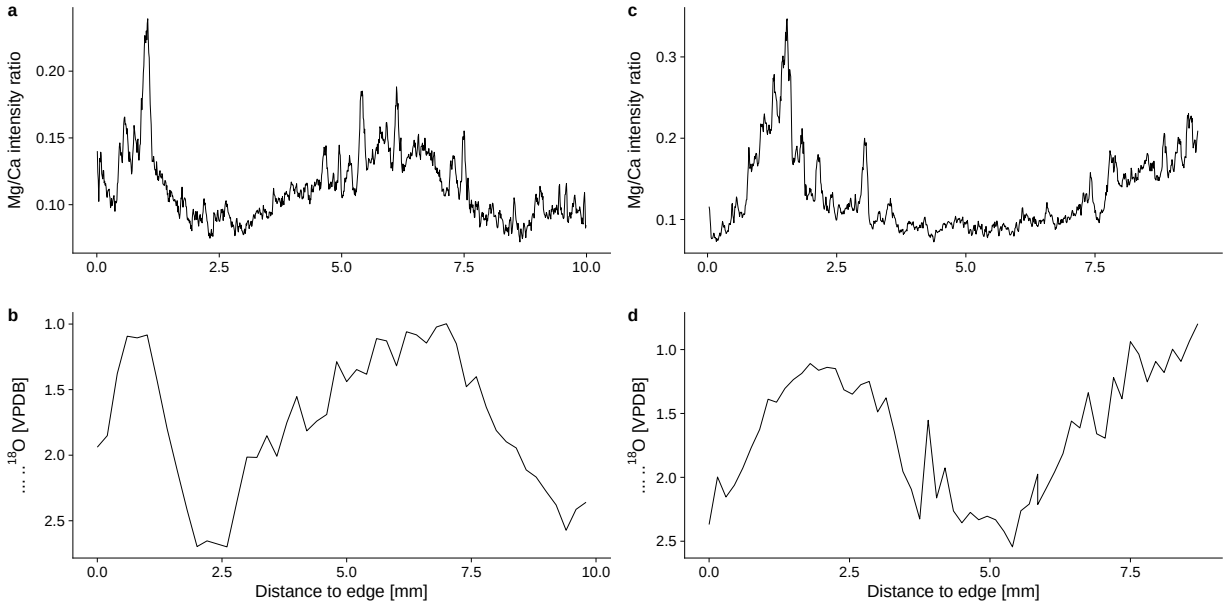

Figure 8: Comparison of LIBS line-scan and sequential ^{18}O-values of specimen ORK-LT5

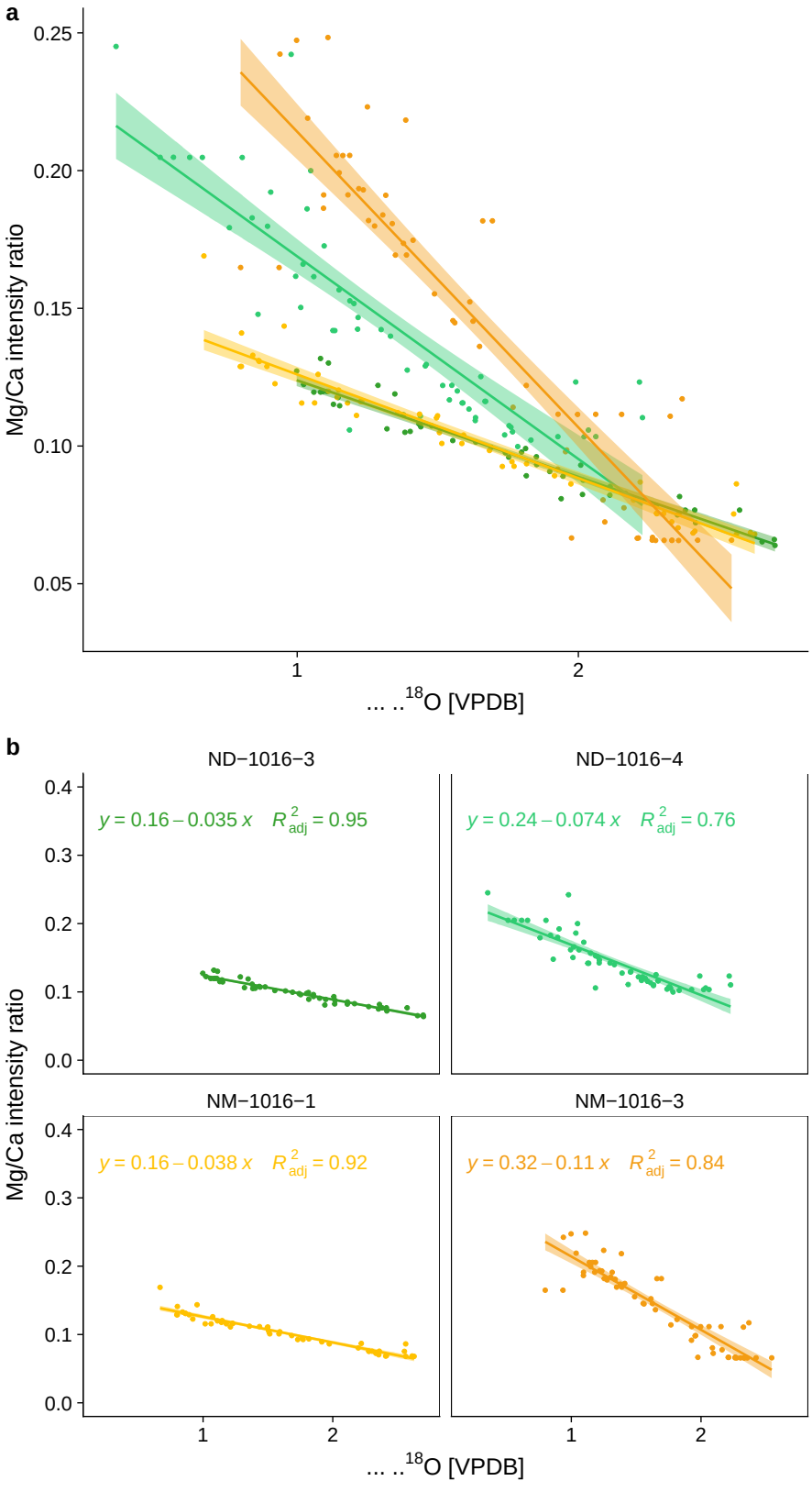

Figure 9: Correlation graphs for *Nacella* sp. specimens

4. Discussion

4.1. Other correlations

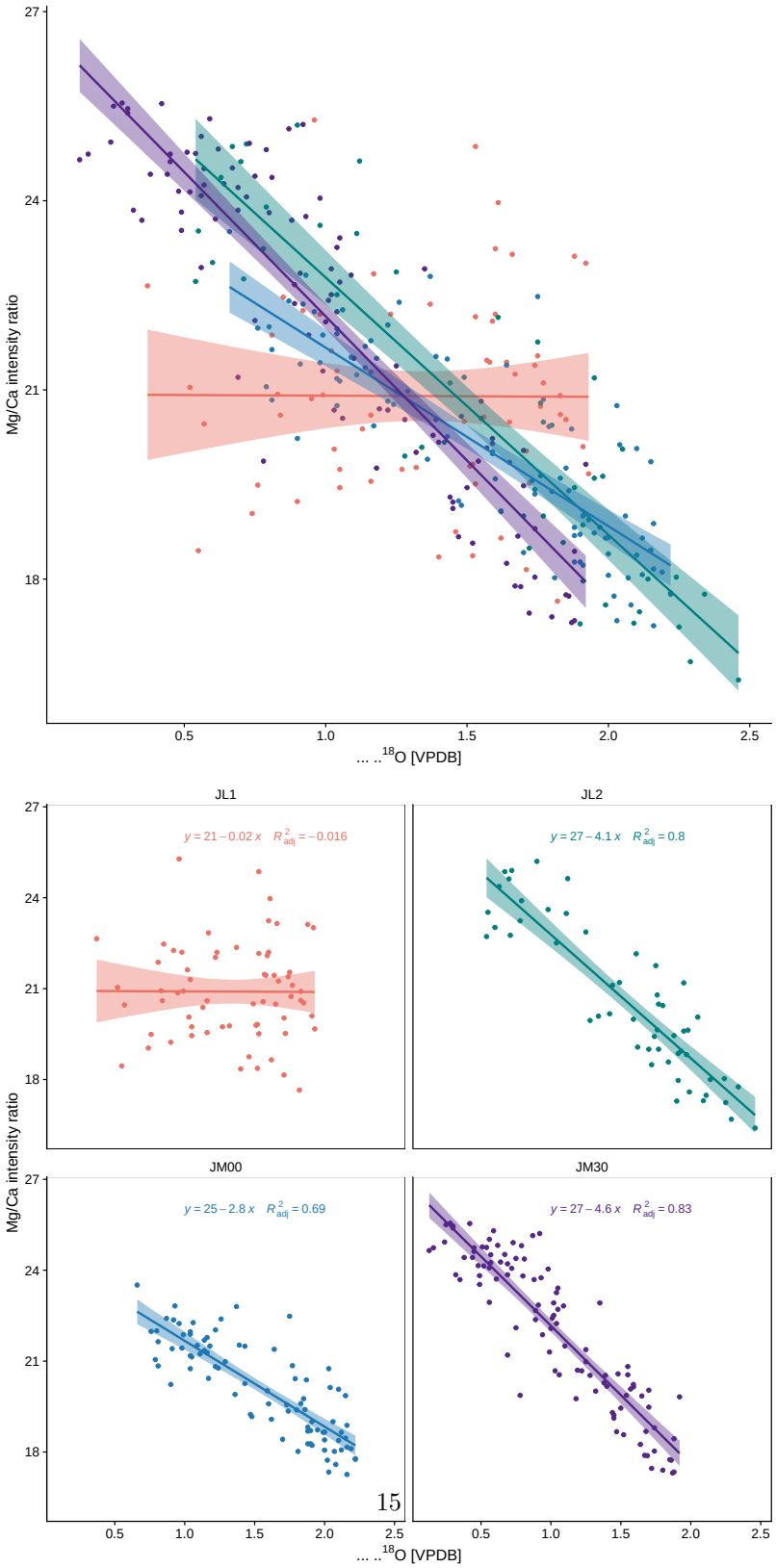

Figure 10: Correlation graphs for Ferguson et al. specimens

Table 2: Table 2: Overview of comparative correlations {#tab:correlations}

Species	Locality	Specimen	Correlation R^2	Study
P. depressa	Northern Spain	LAN541	0.87	(García-Escárzaga et al., 2021)
		LAN545	0.86	
		LAN554	0.78	
		LAN559	0.82	
P. caerulea	Croatia	ISTPC1	0.9	(Hausmann et al., 2019)
		ISTPC2	0.84	
	Crete	AF1911A	0.91[1]	
		AF3003A	0.92[2]	
	Israel	AKKPC2	0.96	
		AKKPC3	0.89	
		FRMPC1	0.84	
		FRMPC2	0.96	
	Libya	MO31A	0.83	
		MP64A	0.33	
		MP67A	0.96	
		MP68A	0.81	
	Malta	MA10	0.82	
	Tunisia	TUNPC1	0.81	
		TUNPC2	0.78	
	Turkey	ANTPC1	0.95	
		ANTPC2	0.93	
		KIZPC1	0.94	
		KIZPC2	0.86	
P. rustica	Gibraltar	JL1	0.02	(Ferguson et al., 2011)
		JL2	0.8 (0.79)	
P. caerulea	Gibraltar	JM00	0.69 (0.79)	
		JM30	0.83 (0.79)	
P. vulgata	Orkney	ORK-LT5	not reported, here 0.88	(Graniero et al., 2017) and this study

[1] SST only, no other geochemical data available
[2] SST only, no geochemical data available

4.2. Comparison of ORK-LT5

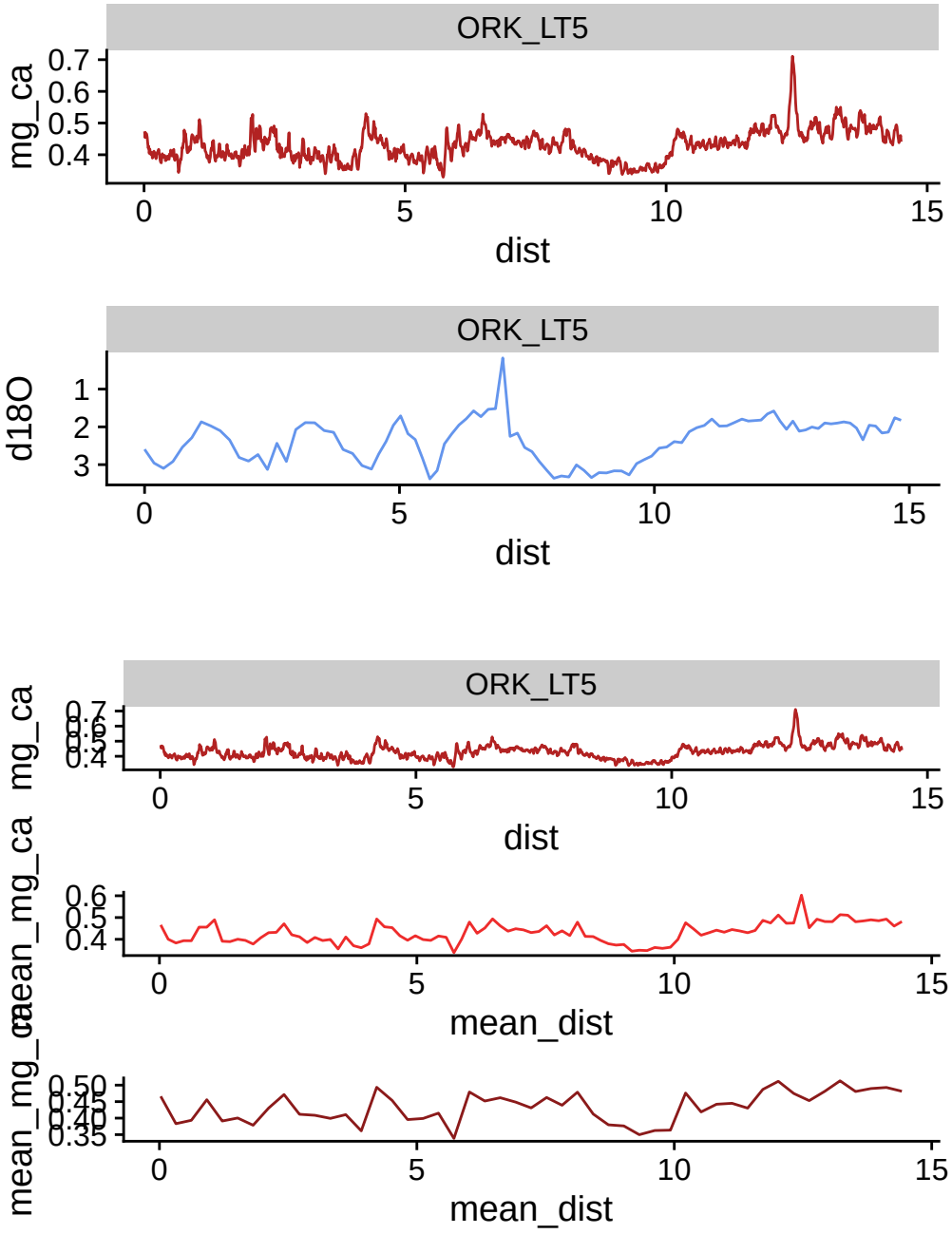

References

Bosch, M.D., Mannino, M.A., Prendergast, A.L., Wesselingh, F.P., O'Connell, T.C., Hublin, J.J., 2018. Year-round shellfish exploitation in the levant and implications for upper palaeolithic hunter-gatherer subsistence. Journal of Archaeological Science: Reports 21, 1198–1214. doi:10.1016/j.jasrep.2017.08.014.

Colonese, A.C., Verdún-Castelló, E., Álvarez, M., Briz i Godino, I., Zurro, D., Salvatelli, L., 2012. Oxygen isotopic composition of limpet shells from the beagle channel: implications for seasonal studies in shell middens of tierra del fuego. J. Archaeol. Sci. 39, 1738–1748. doi:10.1016/j.jas.2012.01.012.

Durham, S.R., Gillikin, D.P., Goodwin, D.H., Dietl, G.P., 2017. Rapid determination of oyster lifespans and growth rates using LA-ICP-MS line scans of shell Mg/Ca ratios. Palaeogeogr. Palaeoclimatol. Palaeoecol. 485, 201–209. doi:10.1016/j.palaeo.2017.06.013.

Fenger, T., Surge, D., Schöne, B., Milner, N., 2007. Sclerochronology and geochemical variation in limpet shells (patella vulgata): A new archive to reconstruct coastal sea surface temperature. Geochem. Geophys. Geosyst. 8.

Ferguson, J.E., Henderson, G.M., Fa, D.A., Finlayson, J.C., Charnley, N.R., 2011. Increased seasonality in the western mediterranean during the last glacial from limpet shell geochemistry. Earth Planet. Sci. Lett. 308, 325–333. doi:10.1016/j.epsl.2011.05.054.

Freitas, P.S., Clarke, L.J., Kennedy, H., Richardson, C.A., 2012. The potential of combined Mg/Ca and δ18O measurements within the shell of the bivalve pecten maximus to estimate seawater δ18O composition. Chem. Geol. 291, 286–293. doi:10.1016/j.chemgeo.2011.10.023.

García-Escárzaga, A., Clarke, L.J., Gutiérrez-Zugasti, I., González-Morales, M.R., Martinez, M., López-Higuera, J.M., Cobo, A., 2018. Mg/Ca profiles within archaeological mollusc (patella vulgata) shells: Laser-Induced breakdown spectroscopy compared to inductively coupled Plasma-Optical emission spectrometry. Spectrochim. Acta Part B At. Spectrosc. 148, 8–15. doi:10.1016/j.sab.2018.05.026.

García-Escárzaga, A., Martínez-Minchero, M., Cobo, A., Gutiérrez-Zugasti, I., Arrizabalaga, A., Roberts, P., 2021. Using Mg/Ca ratios from the limpet patella depressa pennant, 1777 measured by Laser-Induced breakdown spectroscopy (LIBS) to reconstruct paleoclimate. NATO Adv. Sci. Inst. Ser. E Appl. Sci. 11, 2959. doi:10.3390/app11072959.

García-Escárzaga, A., Moncayo, S., Gutiérrez-Zugasti, I., González-Morales, M.R., Martín-Chivelet, J., Cáceres, J.O., 2015. Mg/Ca ratios measured by laser induced breakdown spectroscopy (LIBS): a new approach to decipher environmental conditions. J. Anal. At. Spectrom. 30, 1913–1919. doi:10.1039/C5JA00168D.

Giorgino, T., 2009. Computing and visualizing dynamic time warping alignments in r: The dtw package. Journal of Statistical Software, Articles 31, 1–24. doi:10.18637/jss.v031.i07.

Good, S., Fiedler, E., Mao, C., Martin, M.J., Maycock, A., Reid, R., Roberts-Jones, J., Searle, T., Waters, J., While, J., Worsfold, M., 2020. The current configuration of the OSTIA system for operational production of foundation sea surface temperature and ice concentration analyses. Remote Sensing 12, 720. doi:10.3390/rs12040720.

Graniero, L., Surge, D., Gillikin, D., 2015. Assessing the utility of elemental ratios as a paleotemperature proxy in shells of patelloid limpets, in: EGU General Assembly Conference Abstracts, adsabs.harvard.edu.

Graniero, L.E., Surge, D., Gillikin, D.P., Briz i Godino, I., Álvarez, M., 2017. Assessing elemental ratios as a paleotemperature proxy in the calcite shells of patelloid limpets. Palaeogeogr. Palaeoclimatol. Palaeoecol. 465, Part B, 376–385. doi:10.1016/j.palaeo.2016.10.021.

Hausmann, N., Prendergast, A.L., Lemonis, A., Zech, J., Roberts, P., Siozos, P., Anglos, D., 2019. Extensive elemental mapping unlocks Mg/Ca ratios as climate proxy in seasonal records of mediterranean limpets. Scientific Reports 9, 3698. doi:10.1038/s41598-019-39959-9.

Hausmann, N., Siozos, P., Lemonis, A., Colonese, A.C., Robson, H.K., Anglos, D., 2017. Elemental mapping of Mg/Ca intensity ratios in marine mollusc shells using laser-induced breakdown spectroscopy. J. Anal. At. Spectrom. 32, 1467–1472. doi:10.1039/C7JA00131B.

Hausmann, N., Theodoraki, D., Piñon, V., Siozos, P., Lemonis, A., Anglos, D., 2023. Applying laser induced breakdown spectroscopy (LIBS) and elemental imaging on marine shells for archaeological and environmental research. Sci. Rep. 13, 19812. doi:10.1038/s41598-023-46453-w.

Inall, M., Gillibran, Griffiths, C., MacDougal, N., Blackwell, K., 2009. On the oceanographic variability of the North-West european shelf to the west of scotland. J. Mar. Syst. 77, 210–226. doi:10.1016/j.jmarsys.2007.12.012.

Martínez-Minchero, M., Cobo, A., Méndez-Vicente, A., Pisonero, J., Bordel, N., Gutiérrez-Zugasti, I., Roberts, P., Arrizabalaga, Á., Valdiande, J., Mirapeix, J., López-Higuera, J.M., García-Escárzaga, A., 2022. Comparison of Mg/Ca concentration series from patella depressa limpet shells using CF-LIBS and LA-ICP-MS. Talanta 251, 123757. doi:10.1016/j.talanta.2022.123757.

Nicastro, A., Surge, D., Briz i Godino, I., Álvarez, M., Schöne, B.R., Bas, M., 2020. High-resolution records of growth temperature and life history of two nacella limpet species, tierra del fuego, argentina. Palaeogeogr. Palaeoclimatol. Palaeoecol. 540, 109526. doi:10.1016/j.palaeo.2019.109526.

Ortiz, J.E., Gutiérrez-Zugasti, I., Torres, T., González-Morales, M., Sánchez-Palencia, Y., 2015. Protein diagenesis in patella shells: Implications for amino acid racemisation dating. Quat. Geochronol. 27, 105–118. doi:10.1016/j.quageo.2015.02.008.

Parker, W., Yanes, Y., Mesa Hernández, E., Hernández Marrero, J.C., Pais, J., Soto Contreras, N., Surge, D., 2018. Shellfish exploitation in the western canary islands over the last two millennia. Environ. Archaeol. , 1–23doi:10.1080/14614103.2018.1497821.

Poulain, C., Gillikin, D.P., Thébault, J., Munaron, J.M., Bohn, M., Robert, R., Paulet, Y.M., Lorrain, A., 2015. An evaluation of Mg/Ca, Sr/Ca, and Ba/Ca ratios as environmental proxies in aragonite bivalve shells. Chem. Geol. 396, 42–50.

R Core Team, 2020. R core team r: a language and environment for statistical computing. Foundation for Statistical Computing .

Schöne, B.R., Zhang, Z., Jacob, D., Gillikin, D.P., Tütken, T., Garbe-Schönberg, D., Soldati, A., 2010. Effect of organic matrices on the determination of the trace element chemistry (mg, sr, Mg/Ca, Sr/Ca) of aragonitic bivalve shells (arctica islandica)—comparison of ICP-OES and LA-ICP-MS data. Geochem. J. 44, 23–37.

Shackleton, N.J., 1973. Oxygen isotope analysis as a means of determining season of occupation of prehistoric midden sites.

Archaeometry 15, 133–141.
Surge, D., Barrett, J.H., 2012. Marine climatic seasonality during medieval times (10th to 12th centuries) based on isotopic records in viking age shells from orkney, scotland. Palaeogeogr. Palaeoclimatol. Palaeoecol. 350-352, 236–246. doi:10.1016/j.palaeo.2012.07.003.
Surge, D., Lohmann, K.C., 2008. Evaluating Mg/Ca ratios as a temperature proxy in the estuarine oyster, crassostrea virginica. J. Geophys. Res. 113, G02001. doi:10.1029/2007JG000623.
Vihtakari, M., Ambrose, Jr., W.G., Renaud, P.E., Locke, V, W.L., Carroll, M.L., Berge, J., Clarke, L.J., Cottier, F., Hop, H., 2017. A key to the past? element ratios as environmental proxies in two arctic bivalves. Palaeogeogr. Palaeoclimatol. Palaeoecol. 465, Part B, 316–332. doi:10.1016/j.palaeo.2016.10.020.
Wanamaker, Jr, A.D., Kreutz, K.J., Wilson, T., Borns, Jr, H.W., Introne, D.S., Feindel, S., 2008. Experimentally determined Mg/Ca and Sr/Ca ratios in juvenile bivalve calcite for mytilus edulis: implications for paleotemperature reconstructions. Geo-Mar. Lett. 28, 359–368. doi:10.1007/s00367-008-0112-8.
Wang, T., Surge, D., Mithen, S., 2012. Seasonal temperature variability of the neoglacial (3300–2500 BP) and roman warm period (2500–1600 BP) reconstructed from oxygen isotope ratios of limpet shells (patella vulgata), northwest scotland. Palaeogeogr. Palaeoclimatol. Palaeoecol. 317, 104–113.
Zangrando, A.F., Borrazzo, K.B., Tivoli, A.M., Alunni, D.V., Martinoli, M.P., 2014. El sitio heshkaia 35: nuevos datos sobre la arqueología de moat (tierra del fuego, argentina). Rev. Mus. Antropol. , 11–24doi:10.31048/1852.4826.v7.n1.9090.
Zangrando, A.F.J., Tivoli, A.M., Alunni, D.V., Pérez, S.A., Martinoli, M.P., Vargas, G.P., 2021. Exploring shell midden formation through tapho-chronometric tools: A case study from beagle channel, argentina. Quat. Int. 584, 33–43. doi:10.1016/j.quaint.2020.04.050.